THERMAL CONDUCTIVITY OF REINFORCED GEOPOLYMER FOAMS

#VAN SU LE*, PAVLÍNA HÁJKOVÁ*, **, VLADIMIR KOVACIC*, TOTKA BAKALOVA*, VOLESKÝ LUKÁŠ*,
CHI HIEP LE*, KEVIN CECCON SEIFERT*,***, AMANDA PEREIRA PERES*,***, PETR LOUDA*

*Faculty of Mechanical Engineering, Department of Material Science, Technical University of Liberec,
Studentská 2, 461 17 Liberec, Czech Republic
**Unipetrol Centre for Research and Education,
Revoluční 84, 400 01 Ústí nad Labem, Czech Republic
*** Department of Mechanical Engineering, Federal University of Rio Grande do Sul,
Rua Sarmento Leite, no 425 – centro, Porto Alegre, RS, Cep 90050 – 170, Brazil

#E-mail: longsuvp90@gmail.com

Submitted March 28, 2019; accepted May 27, 2019

Reinforced geopolymer foams were studied in this work as potential building materials. It has been widely assumed that for a given thermal conductivity λ [$W \cdot m^{-1} \cdot K^{-1}$], geopolymer foams can have a lighter density than other materials. The study sought to test this assumption by comparing the thermal conductivity between geopolymer foams. The thermal conductivity λ was measured using an ISOMET 2014 device. In all the experiments, the geopolymer foams were obtained by adding aluminium powder and several combinations: silica fume and fine sand reinforced by short basalt fibres. Curing was carried out at room temperature and then in a furnace at 70 °C. After the curing process, the properties of the samples were tested at 7 and 28 days. The results show that the thermal conductivity, porosity, compressive strength, flexural strength and density for all of the tests ranged in the following values: 0.13 - 0.359 $W \cdot m^{-1} \cdot K^{-1}$; 41.8 - 62.5 %; 1.94 - 9 MPa; 0.96 - 2.93 MPa; 546 - 1028 $kg \cdot m^{-3}$, respectively. It was proven that the filler in the geopolymer foams has a significant influence on the mechanical and physical properties of the tested samples.

INTRODUCTION

Geopolymer foams (GFs) have been widely investigated because of their unique properties, such as low thermal conductivity (TC), good mechanical properties, excellent high temperature stability [1], environmentally friendly, simple fabrication and lower sintering temperature [2-5]. Geopolymers were specified by Joseph Davidovits in the 1970s as a new class of 3-dimensional aluminosilicate materials. [6] Geopolymer materials have a number of advantages, such as excellent mechanical properties, good fire resistance and thermal stability, and they are resistant to acid attacks. A low density geopolymer can be considered as a potential material for applications in many fields. They have been used as thermal insulation, building materials [3, 7, 8], membranes and membrane supports [9, 10], adsorbents and fillers [11-14] or catalysts [15, 16]. Due to its low TC, geopolymers are designed for fire-resistance, which can be exposed to high temperature for an extended period of time [6, 17].

Nowadays, cement is very popular in the construction industry. The global cement production is expected to increase from 3.27 billion metric tonnes in 2010 to 4.83 billion metric tonnes in 2030 [18]. One of the weaknesses of cement is its low fire-resistance compared to some other materials, and it causes a global warming effect. The production of one tonne of cement generates one tonne of carbon-dioxide. That is a reason why a substitute for cement should be developed. Geopolymers are a good candidate for this, because they offer great properties, such as green materials, low cost and durability, low global warming potential (GWP), and excellent fire-resistance [20].

Concrete accounts for a large proportion of weight on a structure. The use of lower density GFs is beneficial in term of reduced structural load bearing with the further benefits of acoustic and thermal insulation [21-23]. However, the mechanical strength is strongly related to the density and low-density geopolymers can exhibit acceptably low strength. Sufficient mechanical strengths can be achieved with the controlled addition of foaming agents in order to achieve an optimum density and pore structure. Different foaming agents can be used to synthesise low-density geopolymers. Metallic aluminium powder is commonly used, which is very reactive in alkaline environments [22, 24, 25].

Fibre reinforcement has been used in various hardened binders to improve the mechanical properties [26-30]. Basalt fibres are inorganic and as such have

a much higher melting point (1450 °C) than organic fibres, making them a suitable candidate for high temperature resistant geopolymer composites [31-34]. Composite materials based on geopolymer matrices can be produced for various applications requiring good performances at elevated temperatures, but also for applications where thermal insulation at room temperature is necessary.

Foaming methods to reduce the density of the geopolymer have been investigated, as low density geopolymers are increasingly being reported in literature as effective in improving the insulating properties [35]. It was found that the addition of more metal powders to the foamed geopolymer resulted in a lower TC, which is caused by the higher porosity [36]. The macrospores are developed thanks to the release of gaseous hydrogen as a result of the aluminium reaction in the strong alkaline environment [24]. Meanwhile, two criteria were considered in selecting the mixtures for the TC testing:

● Mixtures with a compressive strength higher than 2 MPa;

● Mixtures with a bulk density lower than 1100 kg·m^{-3}.

The lowest TC performance (0.132 W·m^{-1}·K^{-1}) was recorded for the one-part geopolymer mortars and 1.2 % Al. Furthermore, a close value of the TC was measured for the same mixture with the 1.5 % aluminium powder [37]. The aluminium powder was used to create bubbles in the porous structure and provide information for the porous geopolymer production. It was introduced by adding the 0.05 - 1 % aluminium powder as a reactive material in the geopolymers to react with the water inside those materials and generate hydrogen gas inside the specimens [38, 39]. The TC diminished from 1.65 to 0.47 W·m^{-1}·K^{-1} for the density from 1800 to 600 kg·m^{-3} [40]. The addition of silica fume as a pore forming agent with an optimum at 5 - 10 wt. % [24] was used. The compressive strength of the geopolymer matrix without the basalt fibre added samples aged 28 days was 35 MPa which increased significantly by 37 percent when only the weight increase of 10 wt. % of basalt fibres were added [41]. As such, the thermal and fire resistance properties of the foamed geopolymers containing the fibre reinforcement were also investigated [33]. The TC measurements should be made at a certain moisture and humidity level for the same batch, as the moisture in the samples has a significant influence on the measurement [33].

This study has been undertaken to investigate the thermal, physical and mechanical properties of geopolymer foamed materials with and without fillers. Evaluating these properties is important for better manufacturing processes and adequate applications.

EXPERIMENTAL

Materials

The industrially supplied material BAUCIS LK (České Lupkové Závody, a.s, Czech Republic) was a two-component aluminosilicate binder based on metakaolin and activated by potassium alkaline [19]. An aluminium powder (pkchemie Inc., Czech Republic) was used to create pores inside the geopolymer. It had an aluminium content of 99 % and the average grain size was 65 μm [42]. The silica fume (produced by Kema Morava – sanační centrum a. s., Republic of Slovenia) contained 90 % SiO$_2$ and the average grain size was 1 mm [43]. A sand (produced by Sklopísek Střeleč a.s., type ST 03-08) was used with a grain size from 0.3 to 0.8 mm [44]. Two types of basalt fibre (Figure 1), a chopped basalt fibre and a waste ground basalt fibre from recycled mate-rial produced by Basaltex a.s. were used. The basalt fibre had a density of 2900 kg·m^{-3}, and thermal conductivity of 0.027 ÷ 0.033 W·m^{-1}·K^{-1} [45].

This work evaluates the impact of the component addition on the binder of the GFs, when one of them was changed and the other components remaining unchanged.
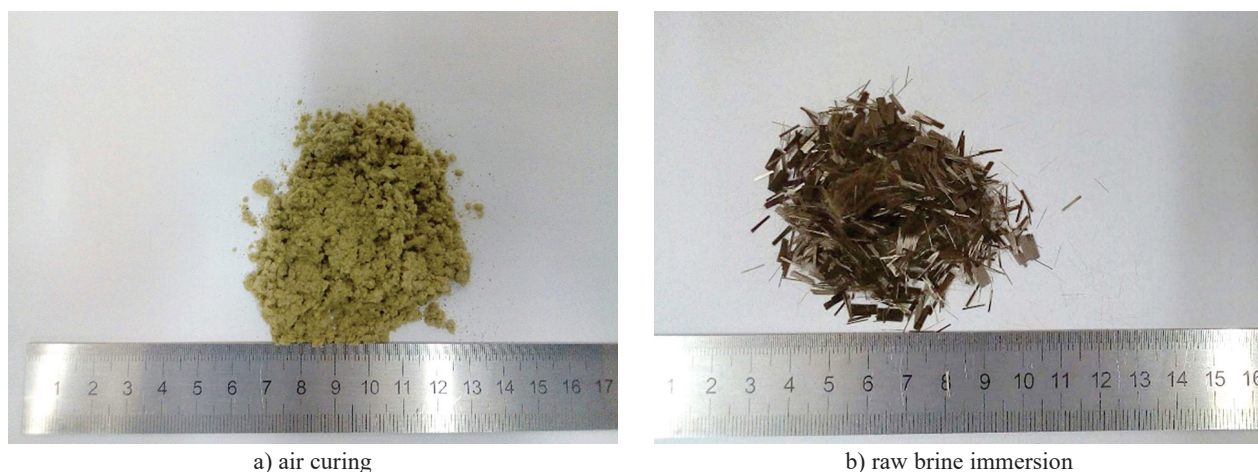

a) air curing   b) raw brine immersion

Figure 1. The waste ground basalt fibres (a), the chopped basalt fibre (b).

Table 1. The composition of the mixtures (all in the ratio of mass).

Mix.	A/B	SF\B	S/B	F1/B	F3/B	Note	Mix.	A/B	SF\B	S/B	F3/B	Note
S1	0.008						S5	0.008	0.026	0.066	0.018	
S2	0.008			0.053			S6	0.008	0.026	0.263	0.018	
S3	0.008			0.158		I	S7	0.008	0.026	0.526	0.018	II
S4	0.008			0.263			S8	0.008	0.026	1.05	0.018	
S9	0.00053	0.026	0.526		0,018		S14	0.008	0.026	0.526	0.0026	
S10	0.0026	0.026	0.526		0,018		S15	0.008	0.026	0.526	0.008	
S11	0.0053	0.026	0.526		0,018	III	S16	0.008	0.026	0.526	0.013	IV
S12	0.008	0.026	0.526		0,018		S17	0.008	0.026	0.526	0.018	
S13	0.016	0.026	0.526		0,018		S18	0.008	0.026	0.526	0.026	

*A – Aluminium Powder Agent, B – Activator LK/Baucis = 0.9 (ratio according to manufacturer), SF – Silica Fume, S – Sand, F1 – Waste Ground Basalt Fibres, F3 – Chopped Basalt Fibres.

The "Note" shown in Table 1:

I: A change in the content of the waste ground basalt fibres and chopped basalt fibres without changing the binder

II: The component of the GFs with a different concentration of the sand and constant other components (binder, silica fume, aluminium powder and chopper basalt fibres)

III: The component of the GFs with a different concentration of the aluminium powder and other constant components (binder, silica fume, sand and chopped basalt fibres)

IV: The component of the GFs with a different concentration of the chopped basalt fibres and other constant components (binder, silica fume, aluminium powder and sand)

Sample preparation

The preparation of the GF samples was made as follows: first, the geopolymer binder was prepared by mixing a potassium activator, which was recommended by the suppliers of the BAUCIS LK, and the mixture was stirred for 5 minutes at room temperature until the solution homogenised. Next, the geopolymer was mixed with different fibres, sand, silica fume content and the mixture were homogenised for a further 5 minutes. The aluminium powder was then added at the end of the mixture preparation for about one minute at high speed. Directly after mixing, the fresh GFs were cast into moulds. The geopolymer foam formation was allowed to stabilise after 2h to 4 h (depending on the composition). The samples were then covered by plastic sheets, cured at 70 °C for 24 h, aged for 27 days at room temperature, and then demoulded for testing and characterisation.

Characterisation of the test methods and the samples for measuring

The flexural strength was measured three times for each mixture, using prims with a size of $40 \times 40 \times 160$ mm^3 after 28 days at room temperature, and three cubes of 40 mm^3 were cut from the tested prims and used to test the compressive strength. The test was carried out on the Universal Testing Machine INSTRON Model 4202 (the maximum load of the sensor is 10 KN) at a loading speed of 1 mm·min^{-1}. The weight, height, width, and length of each sample was measured to calculate the volume density. For the strength and density measurements, the mean values of three samples for each mixture were used.

The TC λ was measured using an ISOMET 2014 device. The measurement was based on the analysis of the temperature response of the analysed material to the heat flow impulses. It was equipped with various planar or probes and a planar probe with a range of 0.015 to 6 W·m^{-1}·K^{-1}. The specimens were cast in moulds of 160×160×40 mm^3. The samples were covered with a plastic film during setting in a furnace at 70 °C for 24 h. After de-moulding they were cured at room temperature for 6 days before the test.

The pore size distributions of two series of GFs were determined using an AutoPore IV 9510 mercury intrusion porosimeter, which operates at pressures from 0.01 to 414 MPa. All the samples of the tests were used on a $40 \times 40 \times 10$ mm^3 plate.

RESULTS AND DISCUSSION

Effect of the fillers and the basalt waste fibre reinforcement

The compressive strength of the GFs without the addition of the waste basalt fibre (sample S1) was 1.94 MPa which significantly increased by 36 %, 87.6 % and 97.4 % when 5, 15.6, 26.3 % of the waste basalt fibre was added, respectively, while on the other hand, the flexural strength of the GFs without the addition of the waste basalt fibre (sample S1), was 1.04 MPa which significantly increased by 32.7 %, 50.9 % when 15.6, 26.3 % of the waste basalt fibre was added, respectively (Figure 2.) Furthermore, group I has a lower volume density and thermal conductivity compared to the other group (Figure 3). However, their strength is the lowest.

Sample S4 is stronger than group I, while the same thermal conductivity can be found on samples S1 and S4. In group II, the results showed a significant increase in the compressive strength, and the same thing happened when comparing the GFs with the flexural strength. After the samples of the GFs were made with a sand aggregate as a filler, the result of sample S8 showed an increase in the compressive strength of 60 % compared to S5, and 300 % compared to S1 without the sand. Samples S6 and S7 had nearly the same strength value, but the volume density of S7 is larger than S6, while having a lower thermal conductivity. The typical compressive
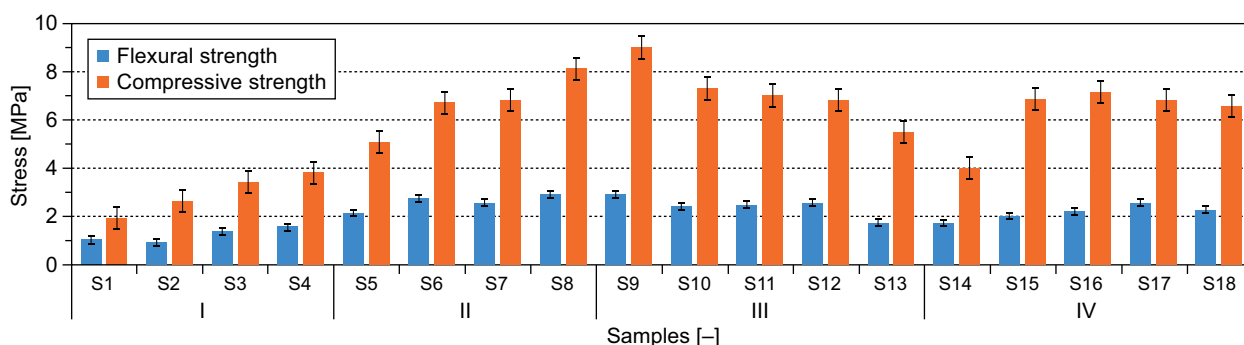

Figure 2. The compressive and flexural strength of the GFs with the reference samples.
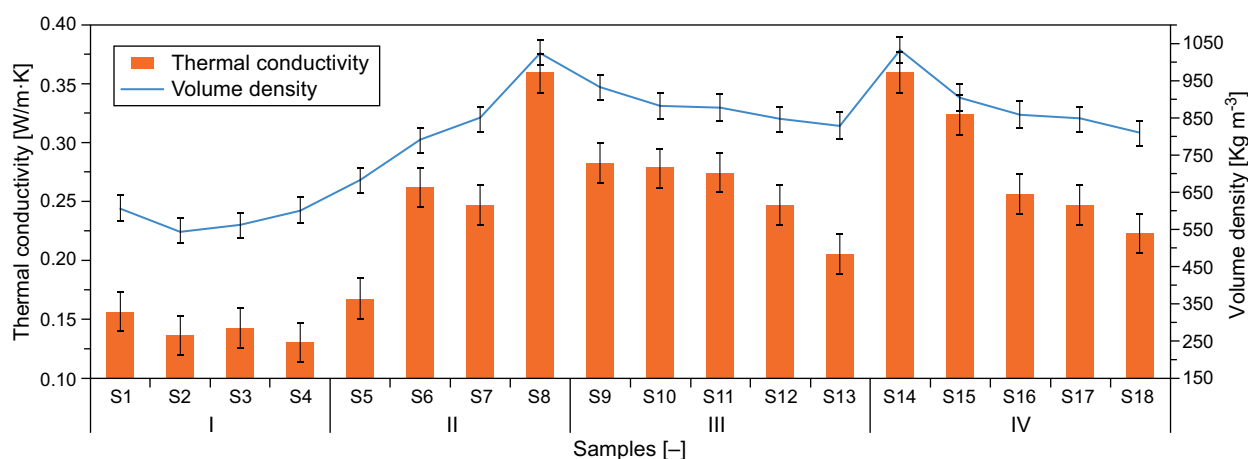

Figure 3. The thermal conductivity and volume density of the GFs with the reference samples.

Table 2. The values of the thermo-physical characteristics of the GFs from this work and literature.

RM	FAT	Density (g·cm⁻³)	Flexural Strength (MPa)	Compressive strength (MPa)	Thermal conductivity (W·m⁻¹·K⁻¹)	Ref.
MK	AL	$0.58 - 1.1$	$0.96 - 2.9$	$2 - 9$	$0.13 - 0.359$	This work
MK	AL, Zn	$0.7 - 1.2$	–	$1 - 7$	$0.17 - 0.55$	[46]
MK	H_2O_2	$0.37 - 0.74$	–	$0.3 - 11.6$	$0.11 - 0.17$	[47]
MK	H_2O_2	$0.3 - 0.58$	–	$0.3 - 4.4$	$0.09 - 0.16$	[1]
MK	Al	$0.36 - 0.59$	–	–	$0.12 - 0.17$	[48]
MK	H_2O_2	$0.3 - 0.6$	–	$1.8 - 5.2$	$0.15 - 0.17$	[3]
MK	SI	$0.3 - 1.1$	–	–	$0.08 - 0.12$	[49]
MK	Al	$0.8 - 1.1$	–	$4.4 - 9.5$	$0.3 - 0.65$	[50]
Mk, FA	H_2O_2	$0.44 - 0.84$	–	$0.3 - 6$	$0.08 - 0.17$	[51]
MK, Glass	H_2O_2	$0.5 - 1.45$	–	$3.1 - 24$	$0.42 - 0.75$	[52]
MK, RHA, VA	Si	$0.36 - 0.47$	–	–	$0.12 - 0.17$	[8]
FA	AL	0.671	1	6	0.145	[5]
FA	Al	$0.89 - 0.93$	–	$5.5 - 10.9$	$0.25 - 0.39$	[53]
FA	H_2O_2	$0.6 - 1.2$	–	$1.2 - 7$	$0.1 - 0.4$	[4]
FA	Al	$0.55 - 0.97$	–	$2 - 8$	$0.1 - 0.25$	[24]
FA, Slag	SAC	$0.6 - 1.2$	–	$2 - 30$	$0.1 - 0.5$	[7]

RW – Raw Materials, FAT – Foam Agent Type, FA – Fly Ash, RHA – Rice Hush Ash, VA – Volcanic Ash, SAC – Surface-Active Concentrate, Ref. – Reference Literature

strength for the GFs with densities of 680 - 1028 kg·m^{-3} is 5 - 8 MPa. The presence of these minerals and aggregates may have provided a better strength. However, our results were high on the thermal conductivity of 0.16 - 0.36 W·m^{-1}·K^{-1} in group III, when the different foaming aluminium powder agent amounts of 0.053, 0.26, 0.53, 0.8 and 1.6 % of mass were added to a binder geopolymer matrix. The compressive strength, volume density and thermal conductivity of the GFs decreased from 10 to 45 %. Sample S8 with a high compressive strength of 9 MPa was achieved within the samples containing 0.053 % aluminium powder. The use of the sand aggregate had a positive effect on the strength for the GFs. Samples S9 to S13 were added at a Baucis ratio: sand 1:1 due to these values, the volume density was around 850 - 950 kg·m^{-3}. The average strength for samples S10, S11 and S12 was around 7 MPa. The addition of aluminium in the GFs had a bigger effect on the porosity, thermal conductivity and volume density. Because sample S13 has used a high amount of aluminium powder, an important decrease in the strength, due to the lack of time to create pores in the GFs, and faster hardening was observed. In group IV, the compressive strength was around 7 MPa except for sample S14, which was determined to be 4.04 MPa. The thermal conductivity and volume density were significantly reduced from 0.36 to 0.2 W·m^{-1}·K^{-1} and from 1028 to 808 kg·m^{-3}, respectively. The values of the thermal conductivity of samples S16 and S17 were the same at around 0.25 W·m^{-1}·K^{-1}. On the other hand, sample S17 had the highest flexural strength of all of the samples in group IV.

Analysis of the micro porosity using an Hg intrusion porosimeter

The pore size distribution in the range of 0.003 - 300 µm, significantly influence the volume of porosity of the GFs when considering the reinforcing fibre, fillers, such as sand, the foaming agent. In Figure 4, it was shown that the volume of the porosity decreases when the basalt waste fibre percentage increases. When it was increased by up to 26.3 % via the weight of the binder (Table 1), it also increased. In Figure 5, it was clearly shown that when the amount of sand decreased, the volume of the porosity also decreased. In Figure 6, the percentage of the aluminium powder on the GFs increased, and, therefore, the volume of the porosity of the GFs also increased.

Analysis of the macro porosity by imaging

In Figure 7, the photographs of the porous samples S1-S4, S5-S8, S9-S13, and S14-S18 are shown. The pores seem irregular in the all of the samples. The reactivity of the foaming agent, the viscosity and homogeneity of

the slurry influence the morphology of the pores (shape and diameter) and their distribution [48]. In Figure 7a, the degree of the pore generation and its size when the percentage of basalt waste fibre was increased can be visually observed. It appears that the size of the largest pores is one cm (Figure 7a). When the percentage of the fillers, such as the sand, increase in the GFs, the pore size is reduced, and the pores become more uniform in diameter (Figure 7b). An increase in the percentage of the aluminium powder or chopped basalt fibre significantly increases the size of the pores, as seen in
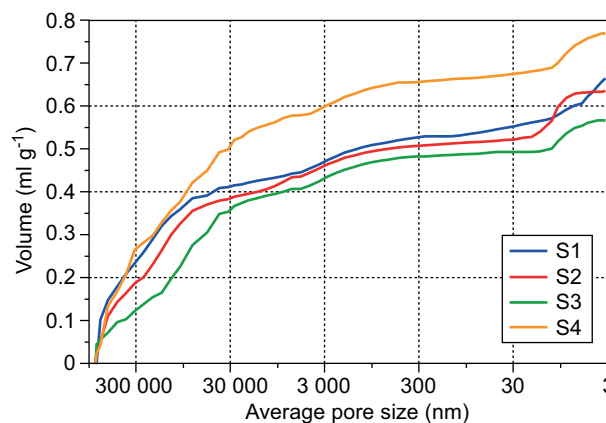

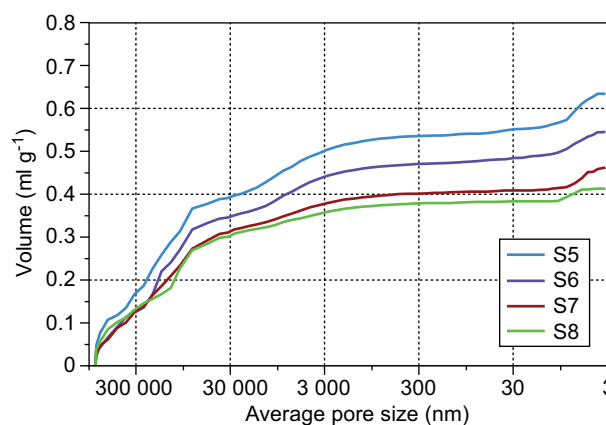Figure 4. The average pore sizes of the different samples S1-S4.

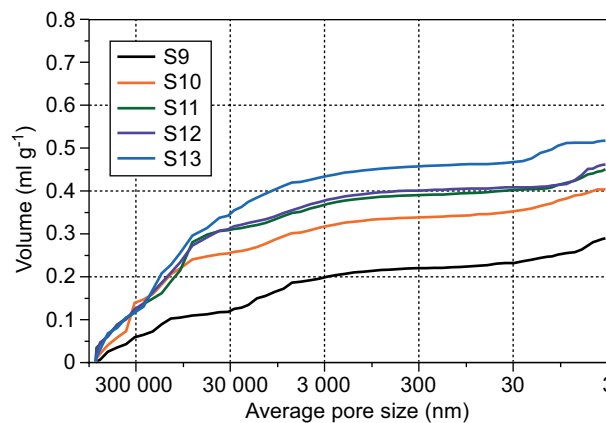Figure 5. The average pore sizes of the different samples S5-S8.

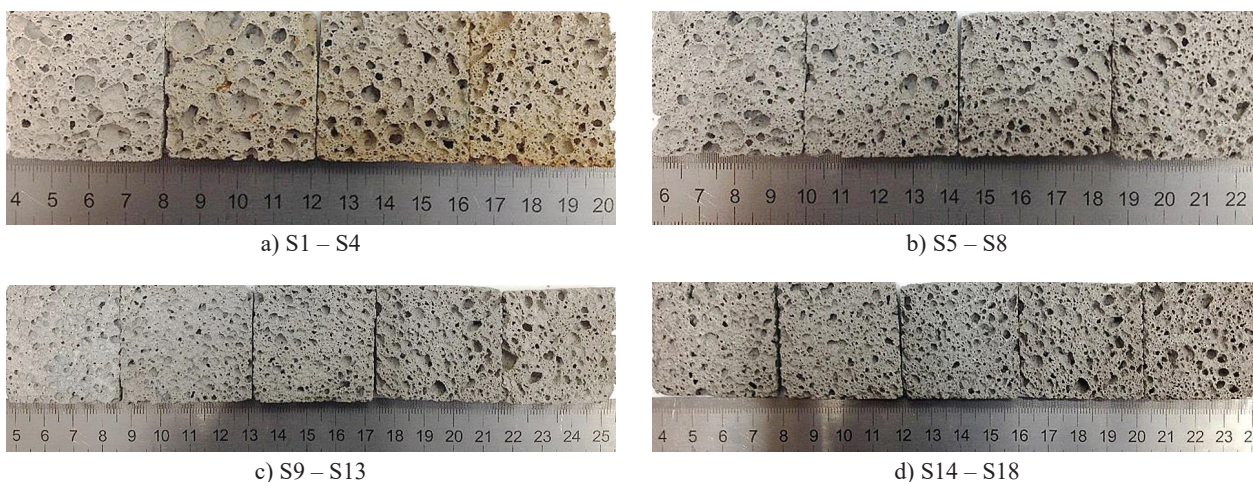Figure 6. The average pore sizes of the different samples S9-S13.

a) S1 – S4

b) S5 – S8

c) S9 – S13

d) S14 – S18

Figure 7. Photos of the different types of GFs with dimension 40×40 mm^2.

Figure 7c and Figure 7d, respectively. Several works can be mentioned to provide an explanation. Larger pores are created in the GFs based on a potassium activator [20]. The low viscosity and the high alkalinity of the slurry help in the creation and coalescence of the H$_2$ bubbles; however, this leads to the fast consolidation of the mixture, thereby, causing the wide statistical distribution of the pore size probability [51]. The circular shape and uniformity of the pore distribution improve the insulating properties of the foams [8, 54]. The broad and heterogeneous distribution of the pores are formed by the intricate network between the porous cavities, which in sum contain a large amount of air This leads to the significant dissipation of the sound waves within the porous matrix [8, 55]. The amount of irregularly formed therein increases the pores considerably. The smaller the formed air voids are, the more regular their shape and homogenous distribution increases the comparable thermal conductivity of the volume density.
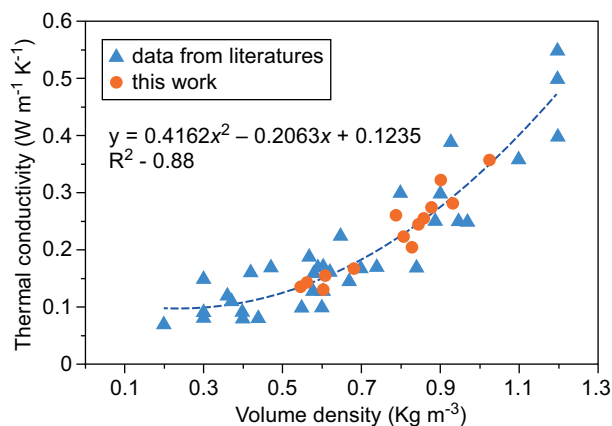

Figure 8. The relationship of the thermal conductivity with the volume density. Data from Ref. [1, 3-5, 7, 8, 33, 45-57] and this work.

Evaluate the relationship between the thermal conductivity and volume density

The exponential trend line with numeric values of $R^2 = 0.88$ shows that the congruent transformation is consistent with the individual measured values. In other words, the increase in the thermal conductivity depends on the volume density. The thermal conductivity also increases with the rising volume density. The values measured in this work are also in accordance with these rules. (Orange curve in Figure 8)

According to the description in Timakulov's work [41], the compressive strength of fly-ash geopolymer was reduced when a 15 - 30 wt. % basalt fibre addition was used. Nonetheless, the results of this work indicate the opposite trend. The concrete's density ranges from 2100 to 2415 kg·m^{-3} [28, 56], while the GFs have a volume density under 1200 kg·m^{-3} (see Table 2 and Figure 8). The thermal conductivity mostly depends on the composition, fillers and testing conditions [57, 58]. This reduction in the strength is due to the fact that the GF needs more aluminium powder in order to achieve large porosity, which decreases the volume density and thermal conductivity. GFs with a wide range of thermal conductivity were successfully synthesised by adding an aluminium powder. Compared to other works [46, 50], where a similar volume density and the same foaming method are shown, the strength and the thermal conductivity indexes do not achieve results as good as those in this work (Table 2). It is evident from the analysis of References 5 and 25 in Table 2 that the result is similar in this work; however, the description in Reference 35 is not in accordance with this work. Furthermore, many heavy metals are contained in the used fly-ash, and these may be hazardous substances that cause health risks [59]. This article shows the possibility to obtain a lower thermal conductivity or a low volume density from a potassium and Baucis (LK) alkaline environment and/or fumed silica and/or fillers

and/or reinforced fibre through the aluminium powder foaming method. The conclusion derived from this work and other literature summarises the dependence on the investigated parameters, such as fibres for reinforcement, fillers and a foaming agent.

The use of a fibre basalt waste as a by-product for reinforcing the GFs combined with the ambient temperature significantly improves the physical, thermal and mechanical properties of the GFs, enabling a reduction in the cost of the GFs and to create an environmentally friendly material. The lowest thermal conductivity of the GFs is 0.13 W·m^{-1}·K^{-1}.

Fillers such as sand, fibres and silica fume as an agent supporting the foaming properties, which improve the properties, were used in the GFs for the reinforcement. This is primarily manifested in the compressive and flexural strengths, whose measured values are around 5 - 9 MPa and 2 - 3 MPa, respectively. The use of silica fume as a waste by-product as an additional ingredient used to obtain the GFs is catalogued according to the risks to the health or the environment as a green material within the current description of the supplier and for concentrated product.

The results of this work allow for the design of the ratio of a proportional mixture (see Table 3).

With the growing demand for housing and of the

Table 3. The composition / information on the ingredients.

Ingredient name	% Wt.	Note
Baucis LK (clay)	41 – 49.6	
Potassium alkaline	37.3 – 44.7	
Fibre waste basalt	13.5 – 20.7	Without fillers
Aluminium	0.62 – 0.68	
Baucis LK (clay)	31.54 – 44.84	
Potassium alkaline	28.39 – 40.36	
Chopper fibres	0.42 – 5.6	
Sand	6.28 – 31.54	With fillers
Silica fume	1.58 – 2.24	
Aluminium powder	0.16 – 0.67	

construction industries in developed and developing countries, the demand for sustainable and friendly materials is increasing, as well as the growing popularity of geopolymers. These materials must be light and be able to withstand heat, have good sound absorption and be durable. Let us look at the common values in Table 2, where the values are shown as the results of this work. It is clear that they allow for the use of the investigated material as a thermal insulation and relative sound insulation.

CONCLUSIONS

The GF characterisation shows that a basalt waste fibre has a significant effect on the mechanical properties of the GFs and the necessary fillers' content.

It has been shown that a higher addition of basalt waste fibres reduces the thermal conductivity of the GFs due to small, homogenised and regular pore distribution.

The results also show that the thermal conductivity is increased after adding fillers with a larger proportion of chopped basalt fibres.

Acknowledgements

REFERENCE

1. C. Bai, G. Franchin, H. Elsayed, A. Zaggia, L. Conte, H. Li, et al., "High-porosity geopolymer foams with tailored porosity for thermal insulation and wastewater treatment," Journal of Materials Research, vol. 32, pp. 3251-3259, 2017. doi: 10.1557/jmr.2017.127

2. I. Lecomte, M. Liégeois, A. Rulmont, R. Cloots, and F. Maseri, "Synthesis and characterization of new inorganic polymeric composites based on kaolin or white clay and on ground-granulated blast furnace slag," Journal of materials research, vol. 18, pp. 2571-2579, 2003. doi: 10.1557/JMR.2003.0360

3. P. Palmero, A. Formia, P. Antonaci, S. Brini, and J.-M. Tulliani, "Geopolymer technology for application-oriented dense and lightened materials. Elaboration and characterization," Ceramics International, vol. 41, pp. 12967-12979, 2015. doi: 10.1016/j.ceramint.2015.06.140

4. R. M. Novais, L. Buruberri, G. Ascensão, M. Seabra, and J. Labrincha, "Porous biomass fly ash-based geopolymers with tailored thermal conductivity," Journal of cleaner production, vol. 119, pp. 99-107, 2016. doi: 10.1016/j.jclepro.2016.01.083

5. P. Hlaváček, V. Šmilauer, F. Škvára, L. Kopecký, and R. Šulc, "Inorganic foams made from alkali-activated fly ash: Mechanical, chemical and physical properties," Journal of the European Ceramic Society, vol. 35, pp. 703-709, 2015. doi: 10.1016/j.jeurceramsoc.2014.08.024

6. J. Davidovits, "years of successes and failures in geopolymer applications. Market trends and potential breakthroughs," in Geopolymer 2002 Conference, 2002, p. 29.

7. Z. Zhang, J. L. Provis, A. Reid, and H. Wang, "Mechanical, thermal insulation, thermal resistance and acoustic absorption properties of geopolymer foam concrete," Cement and Concrete Composites, vol. 62, pp. 97-105, 2015. doi: 10.1016/j.cemconcomp.2015.03.013

8. E. Papa, V. Medri, D. Kpogbemabou, V. Morinière, J. Laumonier, A. Vaccari, et al., "Porosity and insulating properties of silica-fume based foams," Energy and Buildings, vol. 131, pp. 223-232, 2016. doi: 10.1016/j.enbuild.2016.09.031

9. Y. Ge, Y. Yuan, K. Wang, Y. He, and X. Cui, "Preparation of geopolymer-based inorganic membrane for removing Ni^{2+} from wastewater," Journal of hazardous materials, vol. 299, pp. 711-718, 2015. doi: 10.1016/j.jhazmat.2015.08.006

10. C. Bai and P. Colombo, "High-porosity geopolymer membrane supports by peroxide route with the addition of egg white as surfactant," Ceramics International, vol. 43, pp. 2267-2273, 2017. doi: 10.1016/j.ceramint.2016.10.205

11. M. Minelli, V. Medri, E. Papa, F. Miccio, E. Landi, and F. Doghieri, "Geopolymers as solid adsorbent for CO_2 capture," Chemical Engineering Science, vol. 148, pp. 267-274, 2016. doi: 10.1016/j.ces.2016.04.013

12. R. M. Novais, L. Buruberri, M. Seabra, and J. Labrincha, "Novel porous fly-ash containing geopolymer monoliths for lead adsorption from wastewaters," Journal of hazardous materials, vol. 318, pp. 631-640, 2016. doi: 10.1016/j.jhazmat.2016.07.059

13. T. Luukkonen, M. Sarkkinen, K. Kemppainen, J. Rämö, and U. Lassi, "Metakaolin geopolymer characterization and application for ammonium removal from model solutions and landfill leachate," Applied Clay Science, vol. 119, pp. 266-276, 2016. doi: 10.1016/j.clay.2015.10.027

14. F. J. López, S. Sugita, M. Tagaya, and T. Kobayashi, "Metakaolin-based geopolymers for targeted adsorbents to heavy metal ion separation," Journal of Materials Science and Chemical Engineering, vol. 2, p. 16, 2014. doi: 10.4236/msce.2014.27002

15. S. Sharma, D. Medpelli, S. Chen, and D.-K. Seo, "Calcium-modified hierarchically porous aluminosilicate geopolymer as a highly efficient regenerable catalyst for biodiesel production," RSC Advances, vol. 5, pp. 65454-65461, 2015. doi: 10.1039/C5RA01823D

16. Y. J. Zhang, L. C. Liu, Y. Xu, and Y. C. Wang, "A new alkali-activated steel slag-based cementitious material for photocatalytic degradation of organic pollutant from waste water," Journal of hazardous materials, vol. 209, pp. 146-150, 2012. doi: 10.1016/j.jhazmat.2012.01.001

17. M. S. Cilla, P. Colombo, and M. R. Morelli, "Geopolymer foams by gelcasting," Ceramics International, vol. 40, pp. 5723-5730, 2014.

18. The Statistics Portal. (2018). Global Cement Production From 1990 to 2030. Available: https://www.statista.com/statistics/373845/global-cement-production-forecast/

19. a. s. České lupkové závody. (2019). BAUCIS LK. Available: http://www.cluz.cz/en/baucis-lk

20. Z. Abdollahnejad, F. Pacheco-Torgal, T. Félix, W. Tahri, and J. B. Aguiar, "Mix design, properties and cost analysis of fly ash-based geopolymer foam," Construction and Building Materials, vol. 80, pp. 18-30, 2015. doi: 10.1016/j.conbuildmat.2015.01.063

21. Y.-P. Chiu, Y.-M. Lu, and Y.-C. Shiau, "Applying inorganic geopolymers added with aluminium powder to fire-resistant fillers," Materials Research Innovations, vol. 19, pp. S5-642-S5-649, 2015. doi: 10.1179/1432891714Z.0000000001168

22. M. M. A. Abdullah, K. Hussin, M. Bnhussain, K. N. Ismail, Z. Yahya, and R. A. Razak, "Fly Ash-based Geopolymer Lightweight Concrete Using Foaming Agent," International Journal of Molecular Sciences, vol. 13, pp. 7186-7198, Jun 2012. doi: 10.3390/ijms13067186

23. C. Shi, "Composition of materials for use in cellular lightweight concrete and methods thereof," ed: Google Patents, 2002.

24. F. Skvara, R. Sulc, T. Zdenek, S. Petr, S. Vit, and Z. Cílová, "Preparation and properties of fly ash-based geo-polymer foams," Ceramics-Silikaty, vol. 58, pp. 188-197, 2014.

25. A. Hajimohammadi, T. Ngo, P. Mendis, and J. Sanjayan, "Regulating the chemical foaming reaction to control the porosity of geopolymer foams," Materials & Design, vol. 120, pp. 255-265, 2017. doi: 10.1016/j.matdes.2017.02.026

26. T. Alomayri and I. M. Low, "Synthesis and characterization of mechanical properties in cotton fiber-reinforced geopolymer composites," Journal of Asian Ceramic Societies, vol. 1, pp. 30-34, 2013.

27. T. Alomayri, L. Vickers, F. U. Shaikh, and I.-M. Low, "Mechanical properties of cotton fabric reinforced geopolymer composites at 200–1000 C," Journal of Advanced Ceramics, vol. 3, pp. 184-193, 2014. doi: 10.1007/s40145-014-0109-x

28. K. Vijai, R. Kumutha, and B. Vishnuram, "Properties of glass fibre reinforced geopolymer concrete composites," 2012.

29. Š. Hýsek, R. Wimmer, and M. Böhm, "Optimal processing of flax and hemp fibre nonwovens," BioResources, vol. 11, pp. 8522-8534, 2016.

30. Š. Hýsek, M. Podlena, H. Bartsch, C. Wenderdel, and M. Böhm, "Effect of wheat husk surface pre-treatment on the properties of husk-based composite materials," Industrial Crops and Products, vol. 125, pp. 105-113, 2018. doi: 10.1016/j.indcrop.2018.08.035

31. P. Amuthakkannan, V. Manikandan, J. W. Jappes, and M. Uthayakumar, "Effect of fibre length and fibre content on mechanical properties of short basalt fibre reinforced polymer matrix composites," Materials Physics and Mechanics, vol. 16, pp. 107-117, 2013.

32. T. D. Hung, P. Louda, D. Kroisová, O. Bortnovsky, and N. T. Xiem, "New generation of geopolymer composite for fire-resistance," in Advances in Composite Materials-Analysis of Natural and Man-Made Materials, ed: InTech, 2011.

33. G. Masi, W. D. Rickard, M. C. Bignozzi, and A. Van Riessen, "The effect of organic and inorganic fibres on the mechanical and thermal properties of aluminate activated geopolymers," Composites Part B: Engineering, vol. 76, pp. 218-228, 2015. doi: 10.1016/j.compositesb.2015.02.023

34. K. Sakkas, D. Panias, P. Nomikos, and A. Sofianos, "Potassium based geopolymer for passive fire protection of concrete tunnels linings," Tunnelling and underground space technology, vol. 43, pp. 148-156, 2014. doi: 10.1016/j.tust.2014.05.003

35. G. Masi, W. D. Rickard, M. C. Bignozzi, and A. van Riessen, "The influence of short fibres and foaming agents on the physical and thermal behaviour of geopolymer composites," Advances in Science and Technology, vol. 92, p. 56, 2014. doi: 10.4028/www.scientific.net/AST.92.56

36. T.-Y. Yang, C.-C. Chou, and C.-C. Chien, "The effects of foaming agents and modifiers on a foamed-geopolymer," in The 2012 World Congress on Advances in Civil, Environmental, and Materials Research (ACEM'12) Seoul, Korea, 2012.

37. Z. Abodollahnejad, Development Of Foam One-Part Geopolymer. Universidade do Minho Escola de Engenharia, 2016.

38. P. Keawpapasson, C. Tippayasam, S. Ruangjan, P. Thavorniti, T. Panyathanmaporn, A. Fontaine, et al., "Metakaolin-Based Porous Geopolymer with Aluminium Powder," Key Engineering Materials, vol. 608, pp. 132-138, 2014. doi: 10.4028/www.scientific.net/KEM.608.132

39. Z. Q. Guo, X. Li, X. G. Yuan, and H. J. Huang, "Effects of

extrusion methods and powder carriers on powder forming and precursor foaming behavior in the preparation process of aluminum foam," in Advanced Materials Research, 2013, pp. 1734-1739.

40. R. A. Aguilar, O. B. Díaz, and J. E. García, "Lightweight concretes of activated metakaolin-fly ash binders, with blast furnace slag aggregates," Construction and building materials, vol. 24, pp. 1166-1175, 2010. doi: 10.1016/j.conbuildmat.2009.12.024

41. P. Timakul, W. Rattanaprasit, and P. Aungkavattana, "Improving compressive strength of fly ash-based geopolymer composites by basalt fibers addition," Ceramics International, vol. 42, pp. 6288-6295, 2016. doi: 10.1016/j.ceramint.2016.01.014

42. p.-. kovyachemie.cz. (2018). Aluminum powder. Available: https://www.kovyachemie.cz/kontakty/

43. KEMA MORAVA – sanační centrum s.r.o. (2016). KEMA MIKROSILIKA. Available: http://www.kema-morava.cz/files/technicke_listy/CZ%20Kema%20MIKROSILIKA.pdf

44. a. s. Sklopísek Střeleč. (2018). CATALOGUE OF PRODUCTS. Available: https://en.glassand.eu/getFile/case:show/id:432775??

45. B. a.s. (2019). Processing of endless basalt fibers into technical products. Available: http://www.basaltex.cz/cedic/cedic_charakteristika_cz.htm#08

46. Tsung-Yin Yang, Chia-Ching Chou, and a. C.-C. Chien, "the effects of foaming agents and modifiers on a foamed-geopolymer," Advances in Civil, Environmental, and Materials Research (ACEM' 12), 2012.

47. C. Bai, T. Ni, Q. Wang, H. Li, and P. Colombo, "Porosity, mechanical and insulating properties of geopolymer foams using vegetable oil as the stabilizing agent," Journal of the European Ceramic Society, vol. 38, pp. 799-805, 2018. doi: 10.1016/j.jeurceramsoc.2017.09.021

48. E. Kamseu, Z. N. Ngouloure, B. N. Ali, S. Zekeng, U. Melo, S. Rossignol, et al., "Cumulative pore volume, pore size distribution and phases percolation in porous inorganic polymer composites: Relation microstructure and effective thermal conductivity," Energy and buildings, vol. 88, pp. 45-56, 2015. doi: 10.1016/j.enbuild.2014.11.066

49. E. Prud'homme, E. Joussein, and S. Rossignol, "Use of silicon carbide sludge to form porous alkali-activated materials for insulating application," The European Physical Journal Special Topics, vol. 224, pp. 1725-1735, 2015. doi: 10.1140/epjst/e2015-02494-7

50. W. D. Rickard, L. Vickers, and A. Van Riessen, "Performance of fibre reinforced, low density metakaolin geopolymers under simulated fire conditions," Applied Clay Science, vol. 73, pp. 71-77, 2013. doi: 10.1016/j.clay.2012.10.006

51. R. M. Novais, G. Ascensão, L. Buruberri, L. Senff, and J. Labrincha, "Influence of blowing agent on the fresh-and hardened-state properties of lightweight geopolymers," Materials & Design, vol. 108, pp. 551-559, 2016. doi: 10.1016/j.matdes.2016.07.039

52. H. S. Shiu, K. L. Lin, S. J. Chao, C. L. Hwang, and T. W. Cheng, "Effects of foam agent on characteristics of thin-film transistor liquid crystal display waste glass-metakaolin-based cellular geopolymer," Environmental Progress & Sustainable Energy, vol. 33, pp. 538-550, 2014. doi: 10.1002/ep.11798

53. W. D. Rickard and A. Van Riessen, "Performance of solid and cellular structured fly ash geopolymers exposed to a simulated fire," Cement and Concrete Composites, vol. 48, pp. 75-82, 2014. doi: 10.1016/j.cemconcomp.2013.09.002

54. J. Feng, R. Zhang, L. Gong, Y. Li, W. Cao, and X. Cheng, "Development of porous fly ash-based geopolymer with low thermal conductivity," Materials & Design (1980-2015), vol. 65, pp. 529-533, 2015. doi: 10.1016/j.matdes.2014.09.024

55. F. Han, G. Seiffert, Y. Zhao, and B. Gibbs, "Acoustic absorption behaviour of an open-celled aluminium foam," Journal of Physics D: Applied Physics, vol. 36, p. 294, 2003.

56. R. S. Ravindrarajah and W. Jones, "Properties of adjusted density high-performance concrete," Futures in Mechanics of Structures and Materials, p. 351, 2008.

57. Z. Zhang, J. L. Provis, A. Reid, and H. Wang, "Geopolymer foam concrete: An emerging material for sustainable construction," Construction and Building Materials, vol. 56, pp. 113-127, 2014.

58. N. Narayanan and K. Ramamurthy, "Structure and properties of aerated concrete: a review," Cement and Concrete composites, vol. 22, pp. 321-329, 2000. doi: 10.1016/S0958-9465(00)00016-0

59. M. Ahmaruzzaman, "Industrial wastes as low-cost potential adsorbents for the treatment of wastewater laden with heavy metals," Advances in colloid and interface science, vol. 166, pp. 36-59, 2011. doi: 10.1016/j.cis.2011.04.005